

Power Analysis in Multi-layer Graphene Nanoribbon based VLSI Interconnects

Manish Rajani¹

Department of Electronics and Comm. Engineering
Barkatullah University
Bhopal, India
manishrajani999@yahoo.co.in

Sunanda Manke²

Department of Electronics and Comm. Engineering
Barkatullah University
Bhopal, India
mansun12@gmail.com

Abstract—This paper addresses the power dissipation in Multi-layer graphene Nanoribbon (MLGNR) interconnect for VLSI applications at 22nm technology node. Similar analysis is carried out for copper interconnect and results are compared with MLGNR for local, semi-global and global interconnects. SPICE simulation results reveal that power dissipation decreases with increase in Fermi-energy. MLGNR interconnect resistance and inductance increases with decrease in Fermi energy and increase in length. On the other hand, interconnect capacitance is almost independent of Fermi energy and increases with increase in interconnect length. This analysis shows that choice of Fermi energy is critical for good power management.

Keywords—GNR; MLGNR; copper; power; length; Fermi energy; VLSI.

I. INTRODUCTION

With technology scaling, resistivity of copper interconnects is increasing with a high rate due to the combined effect of grain boundary and surface scattering [1],[13]. Graphene Nanoribbon is considered as the attractive candidates for future VLSI interconnects due to its capability to conduct high current densities, high thermal conductivities and large mean free paths [2]-[3]. Graphene Nanoribbon (GNR) can be formed from a mono layer of graphene sheet which consist of carbon atoms packed in a 2D honey comb lattice structure by patterning graphene into a thin strip [3].

GNRs can be classified depending on the shape of their edge (armchair or zigzag). Zigzag GNR's are always metallic and the armchair GNR's can be metallic when $R=3p+2$ or semiconducting when $R=3p$ or $3p+1$, where R is the number of carbon rings along its width and p is an integer [3]. Due to the planar nature of graphene, GNR has straight forward fabrication processes and control over chirality [4] using high resolution lithography [5]. GNR's can be categorized as single-layer GNR (SLGNR) and multi-layer GNR (MLGNR). Due to the lower conductance of SLGNR, MLGNR is preferred for interconnect applications.

Previously, Conductance has been modeled using the simple tight binding model and linear response Landauer formula [6],[7]. Resistance and delay of doped GNR has been compared with other interconnect materials in [6],[8]. Compact physics

based circuit models are developed and delay associated to side contact and top contact MLGNR are compared with copper in [8],[9]. Stability of the GNR has been analyzed in [10] and crosstalk analysis is done for GNR interconnect and compared with copper and multiwall CNT in [11].

In this paper, a complete impedance analysis and power dissipation analysis of MLGNR interconnects is presented and results are compared with copper. The effect of Fermi energy on power dissipation has also been compared. The organization of this paper is as follows. Section I introduces briefs about the structures and properties of GNRs. In Section II, an equivalent RLC model of Multi-layer GNR interconnect is presented. Impedance analysis is done in section III. In section IV, Power is analyzed for local, intermediate and global lengths and compared with that of copper at 22 nm technology node and Section V concludes this work.

II. EQUIVALENT CIRCUIT OF THE MLGNR

The geometry of MLGNR is shown in Fig.1, where H is the thickness, w is the width of the MLGNR, y is the distance from ground plane with ϵ_r as the dielectric constant of its medium, δ is the distance (0.34nm) between the adjacent layers and N is the number of layers.

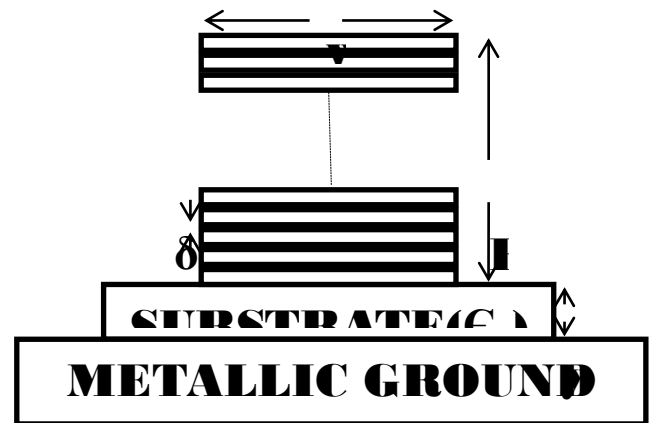


Fig.1. Geometry of MLGNR interconnect.

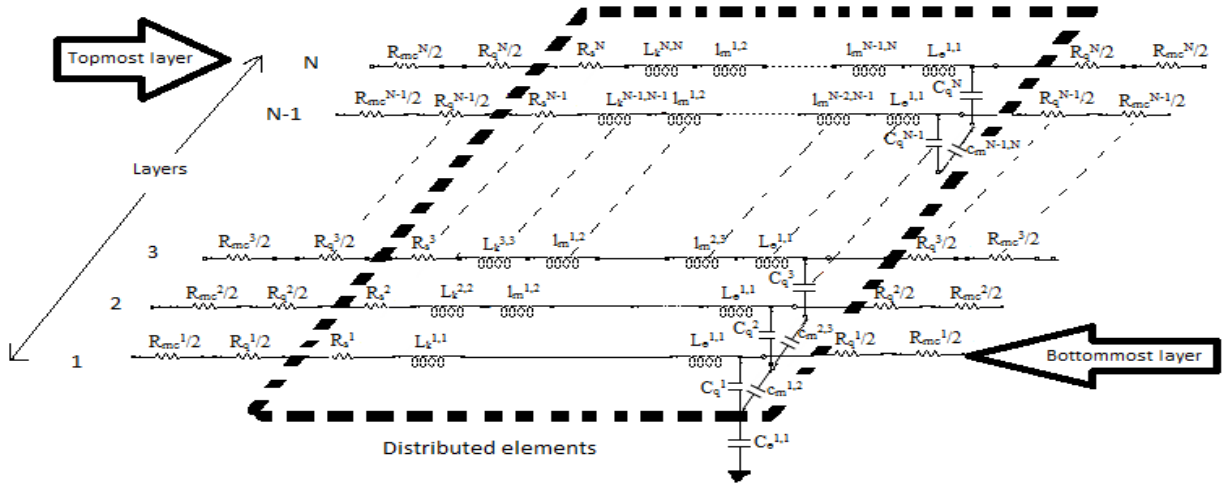


Fig.2. RLC Model for MLGNR interconnect.

The number of layers can be formulated as [11]

$$N = 1 + \text{integer} \left[\frac{H}{\delta} \right] \quad (1)$$

The RLC model of MLGNR interconnect is shown in Fig.2. R_{mc} represents the imperfect contact resistance with its typical value of $20k\Omega$ [12]. R_q is the quantum contact resistance and is defined as [8]

$$R_q = \frac{h/2e^2}{N_{ch}} = \frac{12.9k\Omega}{N_{ch}} \quad (2),$$

where N_{ch} is the number of conducting channels in each layer, h is the Plank's constant and e is the electronic charge. N_{ch} is computed through the occupation probability of states corresponding to the peak and valley of the valence and the conduction subbands and is given by [10]

$$N_{ch} = \sum_{i=1}^{N_c} [1 + e^{(E_i - E_f)/kT}]^{-1} + \sum_{i=1}^{N_v} [1 + e^{(E_i + E_f)/kT}]^{-1} \quad (3),$$

where E_f is the Fermi energy, k is the Boltzmann constant, T is the temperature, v_f is the Fermi velocity, N_c is the density of states of electrons and N_v is the density of states of holes. R_s is the scattering resistance along its length L and is given by [8]

$$R_s = \frac{R_q}{\lambda} / \mu m \quad (4)$$

Hence, the total resistance of the multi-layer GNR is given by

$$R_{eq} = \frac{R_{mc} + R_q + R_s \cdot L}{N} \quad (5)$$

The inductance can be of two types, kinetic inductance (L_k) and magnetic inductance (L_e) [12].

$$L_k = \frac{h/4e^2 \vartheta_F}{N_{ch}} \cong \frac{8nH}{N_{ch}} / \mu m \quad (6)$$

$$L_e = \frac{\mu_0 y}{w} / \mu m \quad (7),$$

where μ_0 is the permeability of free space. The distributed capacitance of GNRs contains both Quantum capacitance (C_q) and electrostatic capacitance (C_e). The quantum capacitance (C_q) per layer is given by [12]

$$C_q = \frac{4e^2/h \cdot N_{ch}}{\vartheta_F} \cong N_{ch} * 0.2fF / \mu m \quad (8)$$

The electrostatic capacitance (C_e) is calculated by using conformal mapping method and is given by [8].

$$C_e = \epsilon M \left[\tanh \left(\frac{\pi w}{4y} \right) \right] \quad (9)$$

$$M(a) = \begin{cases} \frac{2\pi}{\ln \frac{2(1+\sqrt{1-a^2})}{(1-\sqrt{1-a^2})}}, & 0 \leq a < \frac{1}{\sqrt{2}} \\ \frac{2}{\pi} \ln \frac{2(1+\sqrt{a})}{(1-\sqrt{a})}, & \frac{1}{\sqrt{2}} \leq a \leq 1 \end{cases} \quad (10)$$

Mutual inductance (l_m) and mutual capacitance (c_m) exist between each pair of layers and are formulated as [12]

$$l_m = \frac{\mu_0 \delta}{w} / \mu m \quad (11)$$

$$c_m = \frac{\epsilon w}{\delta} / \mu m \quad (12)$$

III. IMPEDANCE ANALYSIS

The per unit length (p.u.l) equivalent impedance parameters of MLGNR are calculated from Eqs.(1)-(12) as a function of Fermi energy. All the physical dimensions of MLGNR and copper are taken from [14],[15] and line parameters (R,L and C) of copper are calculated using appropriate expressions available in [16]. Mean free path (λ) is assumed to be $1\mu\text{m}$ for this analysis [3].

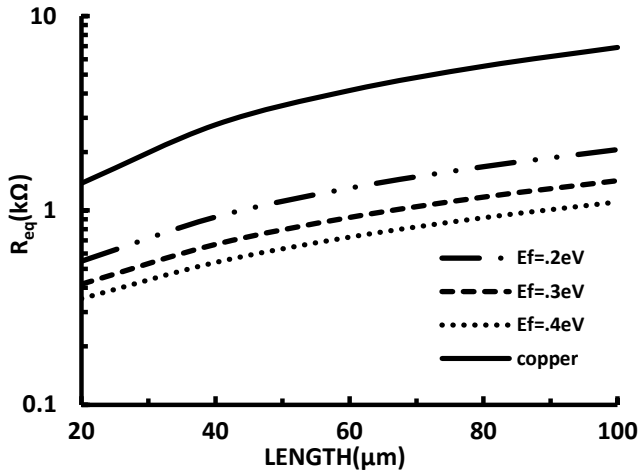


Fig.3(a). Equivalent resistance (R_{eq}) as a function of Fermi energy (E_f) for local lengths of multilayer GNR interconnect.

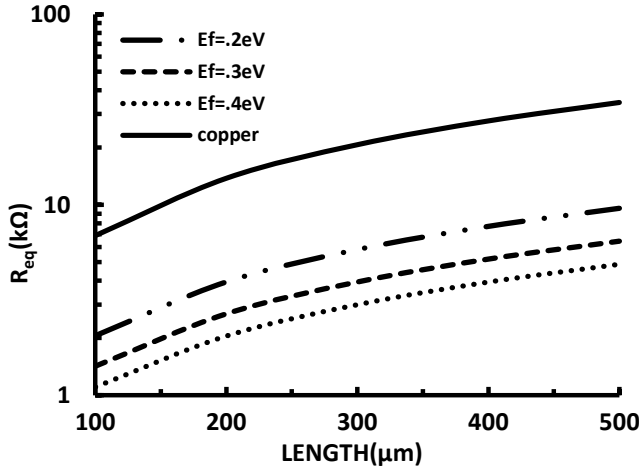


Fig.3(b). Equivalent resistance (R_{eq}) as a function of Fermi energy (E_f) for semi-global lengths of multilayer GNR interconnect.

Figs.3(a)-(c), illustrate a typical example of the dependence of MLGNR interconnect resistance on both length (L) and Fermi energy (E_f) for local, semi-global and global interconnects respectively. It shows that resistance increases with increase in interconnect length for both MLGNR and copper interconnects.

Copper interconnects are of a higher resistance than MLGNR interconnects. Resistance of MLGNR with smaller fermi energies (E_f) is observed more. Furthermore, the rate of increase in resistance with length for both copper and MLGNR interconnects for local and semi-global lengths (see Figs.3(a)-3(b)) is larger than global lengths (see Figs.3(c)).

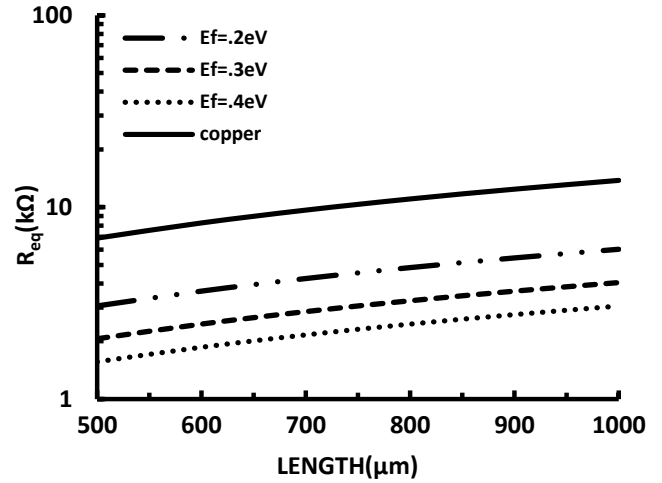


Fig.3(c). Equivalent resistance (R_{eq}) as a function of Fermi energy (E_f) for global lengths of multilayer GNR interconnect.

Figs.4(a)-(c) show the dependence of MLGNR interconnect inductance (L_{eq}) on both length (L) and Fermi energy (E_f). Due to the effect of inductive coupling between the adjacent layers, Inductance (L_{eq}) in MLGNR interconnects is larger than its copper counterpart. The equivalent Inductance (L_{eq}) of MLGNR increases with increase in interconnect length and decrease in Fermi energy (E_f).

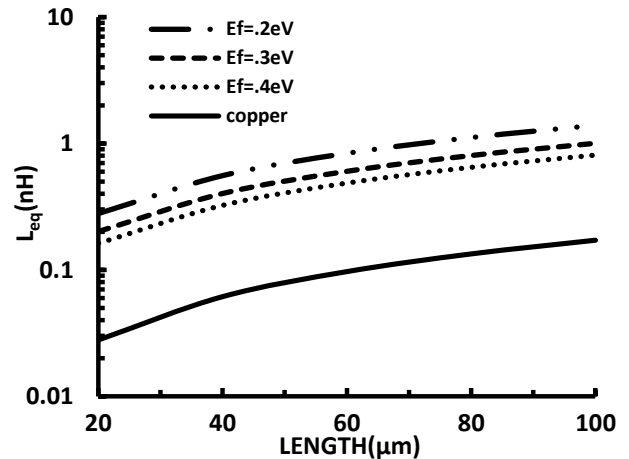


Fig.4(a). Equivalent inductance (L_{eq}) as a function of Fermi energy (E_f) for local lengths of multilayer GNR interconnect.

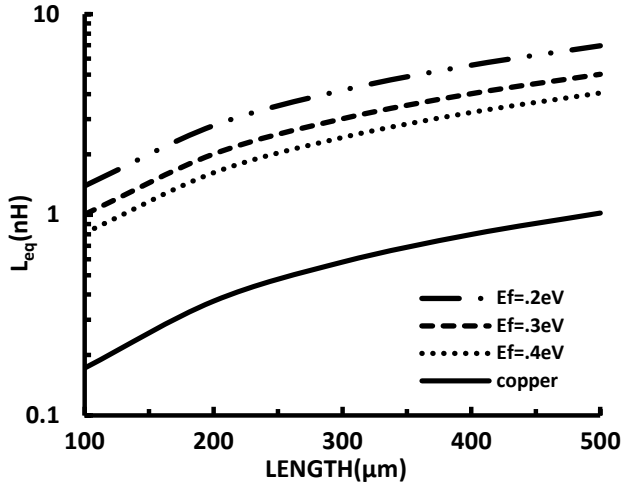


Fig.4(b). Equivalent inductance (L_{eq}) as a function of Fermi energy (E_f) for semi-global lengths of multilayer GNR interconnect.

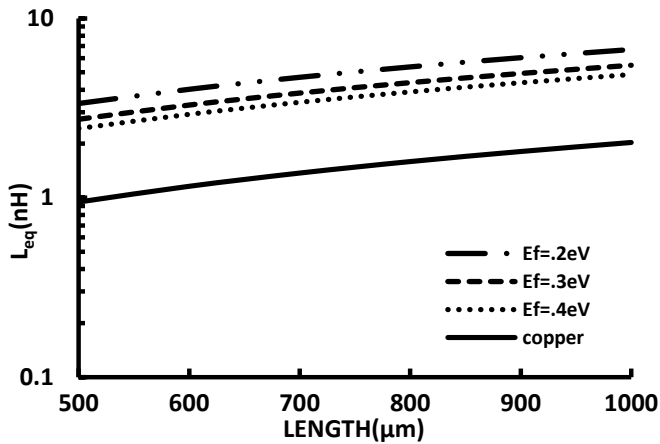


Fig.4(c). Equivalent inductance (L_{eq}) as a function of Fermi energy (E_f) for global lengths of multilayer GNR interconnect.

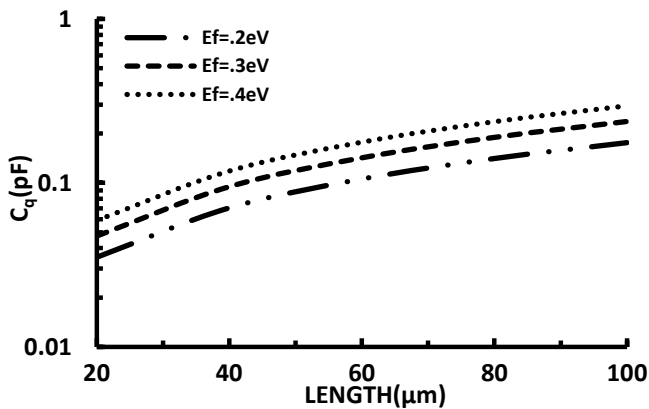


Fig.5(a). Equivalent Quantum capacitance (C_q) as a function of Fermi energy (E_f) for local lengths of multilayer GNR interconnect.

Figs.5(a)-(c) show the dependence of MLGNR interconnect quantum capacitance (C_q) on length and Fermi energy (E_f). The effect of capacitive coupling between the layers is included. The quantum capacitance (C_q) in MLGNR interconnects increases with increase in both length and Fermi energy (E_f).

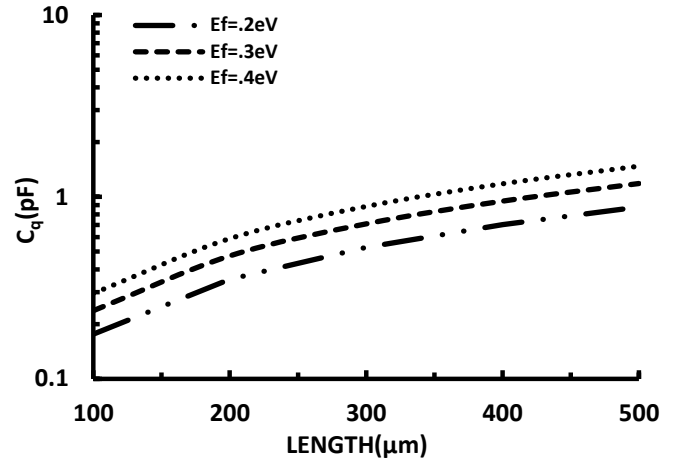


Fig.5(b). Equivalent Quantum capacitance (C_q) as a function of Fermi energy (E_f) for semi-global lengths of multilayer GNR interconnect.

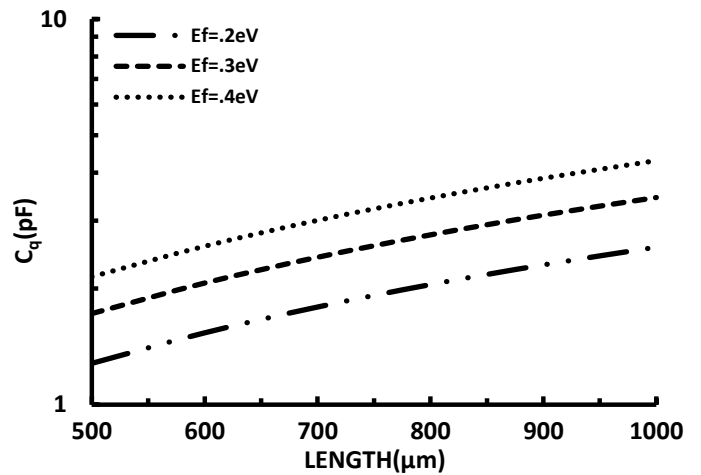


Fig.5(c). Equivalent Quantum capacitance (C_q) as a function of Fermi energy (E_f) for global lengths of multilayer GNR interconnect.

The distributed capacitance is due to quantum capacitance (C_q) and electrostatic capacitance (C_e). In MLGNR interconnects quantum capacitance (C_q) is much larger than electrostatic capacitance (C_e) [7]. The equivalent capacitance is the resultant of the series combination of quantum capacitance (C_q) and

electrostatic capacitance (C_e). The equivalent capacitance in MLGNR interconnect is due to the dominance of lower electrostatic capacitance (C_e) as shown in Table 1.

Table1

S.No.	Lengths	Equivalent capacitance of MLGNR(fF)			Equivalent capacitance of copper(fF)
		$E_f=0.2eV$	$E_f=0.3eV$	$E_f=0.4eV$	
1	Local(20 μ m)	0.503	0.505	0.506	0.1815
2	Semi-Global(500 μ m)	12.59	12.63	12.66	4.538
3	Global(1mm)	22.48	22.53	22.56	14.82

IV. SPICE SIMULATION RESULTS AND DISCUSSIONS

The Simulation setup uses a CMOS inverter driving the MLGNR based equivalent distributed RLC based interconnect having a load of 300fF for local and intermediate lengths and 1pF for global lengths. The input to the inverter is provided by a 0.1 GHz pulse of 1 ns rise time. The performance of this setup is studied by SPICE simulation. The predictive technology model for 22 nm is used for CMOS driver [16]. The equivalent resistance, inductance and capacitance are used for the simulation with optimum number of repeaters. Similar analysis is carried out with copper using the same number of repeaters. The relative measure of MLGNR is obtained by normalizing MLGNR interconnect power by power of copper interconnects. Figs.6(a)-(c) show the variation of power ratios (Normalized power) of multi-layer GNR and copper for local, semi-global and global lengths of interconnect respectively.

Fig.6(a)-(c) shows that power ratios decreases with increase in Fermi energies. Fig.6(a) and Fig.6(b) exemplify that power ratios increases with increase in length nominally. This is due to the combined effect p.u.l resistance and p.u.l capacitance of MLGNR at local lengths and semi-global lengths of interconnect.

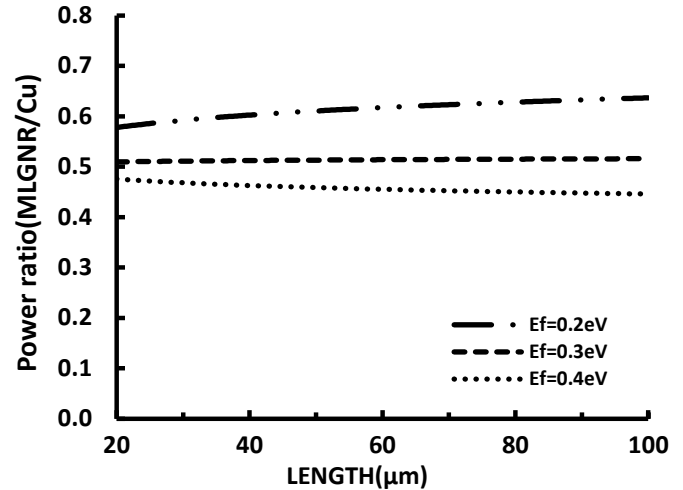


Fig.6(a) Power ratio (MLGNR/Cu) with varying length for local interconnects for different Fermi energies.

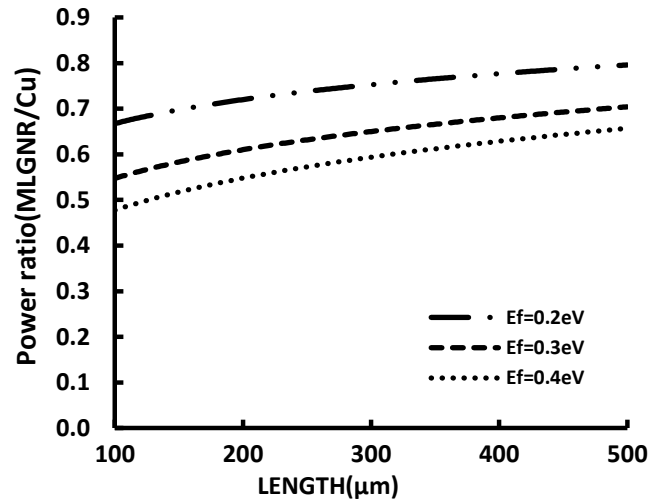


Fig.6(b) Power ratio (MLGNR/Cu) with varying length for semi-global interconnects for different Fermi energies.

Fig.6(c) shows that power ratio decreases with increase in interconnect length as well as Fermi energies (E_f). This is due to the dominance of lower p.u.l. resistance of MLGNR over inductance with approximately unchanged equivalent capacitance for higher values of Fermi energy (see Fig.3 and Table1). It has also been noted that copper interconnects dissipate more power for all interconnect lengths due to larger resistance compared to MLGNR (see Fig.3). Thus, these simulated results further reveal that higher value of Fermi energy should be chosen in case of MLGNR for high speed interconnect applications.

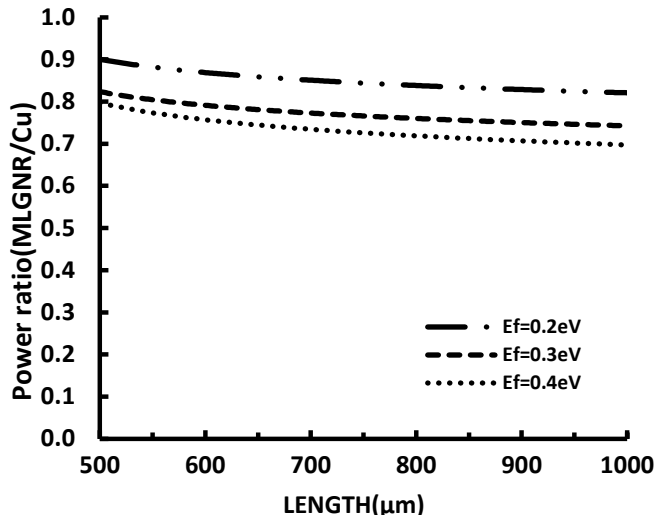


Fig.6(c) Power ratio (MLGNR/Cu) with varying length for global interconnects for different Fermi energies.

V. CONCLUSION

The influence of Fermi energy on power dissipation of MLGNR interconnects critically examined in this paper. SPICE simulation is used to compare MLGNR interconnect powers with that of copper interconnect. The results show that Fermi energy can control the impedance of MLGNR interconnect. This can be utilized to improve power dissipation in MLGNR interconnect. For low power applications larger Fermi energies are preferable.

REFERENCES

- [1] W. Steinhogel et al., "Comprehensive study of the resistivity of copper wires and lateral dimensions of 100nm and smaller," *Journal of Applied Physics*, vol. 97, 023706 (2005).
- [2] A. A. Balandin, S. Ghosh, W. Bao, I. Calizo, D. Teweldebrhan, F. Miao, and C. N. Lau, "Superior thermal conductivity of single-layer graphene," *Nano Lett.*, vol. 8, no. 3, pp. 902–907, Feb. 2008.
- [3] H. Li et al., "Carbon Nanomaterials for Next-Generation Interconnects and Passives: Physics, Status, and Prospects," *IEEE Trans. Electron Devices*, vol. 56, no. 9, 2009, pp. 1799–1821.
- [4] A. Naeemi, J. D. Meindl, "Conductance Modeling for Graphene Nanoribbon (GNR) Interconnects," *IEEE Electron Device Letters* (2007), vol. 28, no. 5, pp. 428–431, May 2007.
- [5] X. Chuan, L. Hong, and K. Banerjee, "Modeling, Analysis, and Design of Graphene Nano-Ribbon Interconnects," *Electron Devices, IEEE Transactions on*, vol. 56, pp. 1567–1578, 2009.
- [6] A. Naeemi and J. D. Meindl, "Conductance modeling for graphene nanoribbon (GNR) interconnects," *IEEE Electron Device Lett.*, vol. 28, no. 5, pp. 428–431, May 2007.
- [7] C. Xu, H. Li, and K. Banerjee, "Graphene nano-ribbon (GNR) interconnects: A genuine contender or a delusive dream?," in *IEDM Tech. Dig.*, 2008, pp. 201–204.

- [8] A.K. Nishad and R. Sharma, "Analytical Time-Domain Models for Performance Optimization of Multilayer GNR Interconnects," *IEEE Journal of selected topics in Quantum Electronics*, vol. 20, no. 1, Jan 2014.
- [9] V. Kumar, S. Rakheja and A. Naeemi, "Performance and Energy per-Bit Modeling of Multilayer Graphene Nanoribbon Conductors," *IEEE Transactions on Electron Devices*, vol. 59, no. 10, pp. 2753–2761, 2012.
- [10] S. H. Nasiri, M. K. M. Farshi, and R. Faez, "Stability analysis in graphene nanoribbon interconnects," *IEEE Electron. Device Lett.*, vol. 31, no. 12, pp. 1458–1460, Dec. 2010.
- [11] D. Das and H. Rahaman, "Crosstalk and Gate Oxide Reliability Analysis in Graphene Nanoribbon Interconnects," in *Electronic System Design (ISED), 2011 International Symposium on*, 2011, pp. 182–187.
- [12] J.-P. Cui, W.-S. Zhao, W.-Y. Yin, and I. Hu, "Signal transmission analysis of multilayer graphene nano-ribbon (MLGNR) interconnects," *IEEE Trans. Electromagn. Compat.*, vol. 53, no. 4, Nov, 2011.
- [13] W. Steinhogel, et al., "Size-dependent Resistivity of Metallic Wires in the Mesoscopic Range," *Physical Review B*, 66, 075414, 2002.
- [14] Hong Li, Wen-Yan Yin, Kaustav Banerjee and Jun-Fa Mao, "Circuit Modeling and Performance Analysis of Multi-Walled Carbon Nanotube Interconnects," *IEEE Transactions on Electron Devices*, vol. 55, no. 6, pp. 1328–1337, 2008.
- [15] International Technology Roadmap for Semiconductors (ITRS) reports, 2006. [Online]. Available: <http://www.itrs.net/reports.html>
- [16] *Predictive Technology Model*, 2008, [Online]. Available: <http://ptm.asu.edu/>.